Delayed Block Transfer Function in the Frequency Domain

Hiroshi Kanai, *Member, IEEE,* Toyohiko Hori, Noriyoshi Chubachi, *Member, IEEE,* and Takahiko Ono

Abstract—**When the impulse response of a transfer system is long, it is difficult for the standard cross spectrum method to obtain an accurate estimate of the transfer function by applying the fast Fourier transform (FFT) with a finite length window. The bias error in the estimate is large especially around the resonant frequency of the transfer system. In this paper, therefore, we propose an alternative new method to obtain an accurate estimate of the transfer function. The delayed block transfer function is introduced to detect the components that are correlated to the signal in the input window but leak from the output window. Based on these transfer functions, the total characteristics of the transfer system are estimated accurately. In the latter half of the paper, we derive the theoretical expressions for the bias errors in the transfer functions estimated by the proposed and the standard methods. By thoroughly comparing the resultant expressions, the superiority and the usefulness of the proposed method are theoretically confirmed. Finally, the simulation experiments show the advantages of the proposed method.**

I. Introduction

THERE has been a dramatic increase in spectrum estimation research activities, especially in the past two decades, since the digital fast Fourier transform (FFT) algorithm was introduced about 25 years ago [1]. The FFT has expanded the role of spectral estimation from research novelty to practical use. Although there are many disadvantages of such FFT-based results, the FFT is most commonly applied to unknown signals in many practical fields before using other parametric techniques because the expanded orthonormal functions employed in the FFT are predetermined and are independent of the signal.

Bingham *et al.* [4] discussed the computationally fastest way to estimate the power spectrum of a time series from the FFT performed directly on the weighted data set. Welch [5] proposed a method for the application of the FFT to the estimation of power spectra, which involves sectioning the records, taking modified periodgrams of these sections, and averaging these modified periodgrams. The weighted overlapped segment averaging is advocated by Nuttall and Carter [37], [41] to give stability and to minimize the impact of window sidelobes. Other references to the FFT and its application for power spectrum estimation may be found in Richards [2], Cochran *et al.* [3], Jenkins and Watt [6], Bertram [8], Glisson *et al.* [9], Cooley *et al.* [10], [11], Oppenheim and Shafer [19], Yuen [29], and Amin [56].

In the power spectrum estimation, leakage effects arising in the frequency domain due to the time domain windowing can be reduced by the selection of windows with nonuniform weighting. Bertram [12] provided a definitive description of the leakage problem. Harris [30] and Nuttall [43] have provided a good summary of the merits of various windows. Nuttall and Carter [46] presented a spectrum estimation method based on lag weighting. Other references include [16], [26], [39], [40], and [53].

As an application of these FFT-based spectrum estimation methods, the coherence function has been developed for a linear measure of causality in the transfer function between a pair of signals. Carter, Knapp, and Nuttall [17], [23] proposed the standard method to estimate the cross spectrum and the coherence function by partitioning the two signals into overlapping segments and computing the power spectrum of each segment via the FFT. The resultant power spectra are then averaged to reduce the bias and variance of the resulting estimates. The coherence function is effective in many fields as pointed out by Carter and Knapp [20], and it has been applied to system identification [17], measuring SNR and linear-to-nonlinear power ratio [17], and determining signal time delay [17], [18], [44]. Knapp and Carter [25] developed a maximum likelihood estimator (MLE) for determining time delay between signals based on the cross correlation, which is identical to one proposed by Hannan and Thomson [15]. A MLE for coherence is derived by Mohnkern [57]. Chan *et al.* [38] proposed a regression approach of the coherence function by solving the discrete Wiener-Hopt equation. Youn *et al.* [45], [47] introduced an adaptive approach based on Widrow's LMS algorithm into the estimation of the coherence function for nonstationary signals. A tutorial review of work in coherence and time delay estimation was presented by Carter [50], [55]. Other references for the estimation of the coherence function or the cross spectrum using the FFT and their applications are found in Jenkins and Watt [6], Carter *et al.* [18], Talbot [22], Blake [28], Piersol [31], Seybert *et al.* [34], Barret [35], Chan [48], Cadzow [51], Cusani [58], and Mansour *et al.* [59]. The error analyses for their estimates are provided by Benignus [7], Bendat [33], Walker [42], Schmidt [49], Mathews *et al.* [52], and Gish *et al.* [54].

For the multiple input/output cases, Bendat [24], [27] provided methods to estimate the transfer function and the coherence function. Other references for the coherence function, partial coherence, and system identification are found in Jenk-

Manuscript received June 10, 1992; revised September 14, 1993. The associate editor coordinating the review of this paper and approving it for publication was Prof. Douglas Williams.

H. Kanai and N. Chubahi are with the Department of Electrical Engineering, Faculty of Engineering, Tohoku University, Sendai, Japan.

T. Hori is with NTT, Japan

T. Ono is with Ono Sokki Company, Ltd., Tokyo, Japan.

IEEE Log Number 9401252.

ins and Watt [6], Bendat and Piersol [13], [36], Dodd *et al.* [21], and Romberg [32].

In the standard method established by these enormous studies in literature, a transfer function is estimated by the ratio of the averaged cross spectrum between the input and output to the averaged input power spectrum. If a time window employed in the FFT is not long enough compared to the length of the transfer system response, however, a bias error due to the insufficiency of the time window length is generated. The cause of the bias error is that the signal in the output window does not contain the whole response to the signal in the input window and contains an extraneous response to the preceding input signal. As the system Q (quality factor) increases, the bias error in the transfer function estimates gets large especially around the resonant frequencies if the window length is kept constant.

A method to determine the window length based on the allowable bias error limit was investigated by Ono *et al.* [60]. A coherence function obtained from the signals in the input window and delayed output window (called *a delayed block coherence function*) is proposed for the detection of a missing signal in the output that is coherent to the input [60]. Based on the theoretical consideration for the delayed block coherence function, a method to estimate the damping factor of a transfer system was presented in [61]. From the estimate of the damping factor, an optimum window length is determined from the allowable bias error limit. It is, however, still difficult to determine an accurate estimate of the transfer function with a long impulse response by these studies.

In this paper, after pointing out these problems in Section II, we propose in Section III a new method to accurately estimate the transfer function when the transfer system has a long impulse response. By thoroughly comparing the accuracy between the estimates obtained by the proposed method and the standard cross spectrum method, we derive theoretical expressions for the estimates of the transfer function in Section IV. From these expressions, the superiority and the usefulness of the proposed method are theoretically and experimentally confirmed in Sections V and VI, respectively.

II. The Standard Estimation Method and its Problems

Let us consider a single input/single output system with extraneous noise at the output point only as shown in Fig. 1. Let us assume that the input measurement $x(t)$ is essentially noise-free, whereas the output measurement $y(t)$ consists of the sum of the ideal linear response $z(t)$ to $x(t)$ and the noise component $n(t)$. Using the discrete expression obtained by sampling each signal at an interval τ, the resultant output measurement is given by

$$\begin{aligned} y(n) &= z(n) + n(n) \\ &= h(n) * x(n) + n(n) \end{aligned} \tag{1}$$

where $*$ indicates a convolution operation, and $h(n)$ is an impulse response of the transfer system, which should be estimated below. Let us assume that the input signal $x(n)$ and the measurement noise $n(n)$ are stationary white noise and mutually uncorrelated. Let the average power of $x(n)$ and $n(n)$ be σ_x^2 and σ_n^2, respectively.

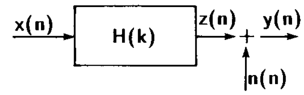

Fig. 1. Signal transmission system model employed in this paper.

By applying an MN-point discrete Fourier transform to the input signal $x(n)$ and the output signal $y(n)$, both of which are windowed, where each window has MN points in length, (1) is written as

$$Y(k) = H(k)X(k) + N(k) \tag{2}$$

where k is an integer representing discrete frequencies, and the discrete spectrum $X(k)$ is given by

$$X(k) = \sum_{n=0}^{MN-1} x(n) \exp\Big(-j2\pi \frac{kn}{MN}\Big). \tag{3}$$

The least squares estimate, which we denote by $\widehat{H_{\mathrm{all}}}(k)$, of the transfer function $H(k)$ in (2) is obtained by the cross spectrum method [13], [36] such as

$$\widehat{H_{\mathrm{all}}}(k) = \frac{E[X^*(k)Y(k)]}{E[|X(k)|^2]}, \quad (k = 0, 1, \ldots, MN-1) \tag{4}$$

where $E[\cdot]$ and * denote the ensemble average and a complex conjugate, respectively. For each frequency, the estimate $\widehat{H_{\mathrm{all}}}(k)$ minimizes the average power $E[|N(k)|^2]$ of the noise component $n(n)$.

If the system response is long compared with the window length, however, the estimate $\widehat{H_{\mathrm{all}}}(k)$ in (4) does not give accurate results. This is due to the following: The estimate $\widehat{H_{\mathrm{all}}}(k)$ of (4) is obtained, assuming that the impulse response to every input pulse in a block is dropped at the end of the block as shown in Fig. 2(a). For example, the responses to the impulses $x(0)$, $x(MN/2)$, and $x(MN-1)$ are estimated so that they have, respectively MN-point, $MN/2$-point, and 1-point in length. These relations between $x(n)$ and $y(n)$ cannot be expressed by a linear system. In the least square estimate of $\widehat{H_{\mathrm{all}}}(k)$ in (4), the nonlinear transfer system is approximated by a linear system. As a result, the bias error in the transfer function estimate $\widehat{H_{\mathrm{all}}}(k)$ becomes larger around the resonant frequencies as the impulse response of the transfer system becomes longer. This bias error is caused even for the case of SNR $= \infty$ and for the case where the average number in (4) is infinite.

III. A New Method of Estimating the Transfer Function

From a different point of view, let us consider the reason the bias error happens in the transfer function, which is estimated by the standard method as follows: Let us divide the input signal $x(n)$ and the output signal $y(n)$ in a section with MN points in length into two blocks ($x_1(n)$ and $x_2(n)$) and ($y_1(n)$ and $y_2(n)$), respectively, where each has $MN/2$ points in length as shown in Fig. 2(b). Using the spectra $X_1(k)$, $Y_2(k)$,

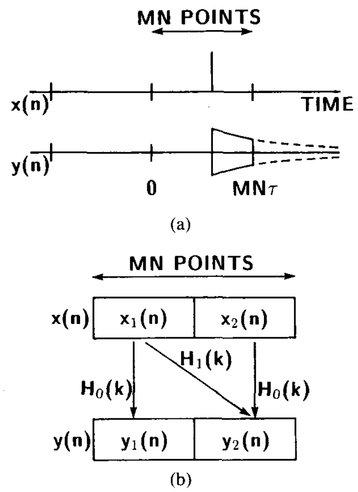

Fig. 2. (a) Impulse response is dropped at the end of the block in the standard method. (b) Illustration explaining the cause of the bias error in the estimates obtained by the standard method.

$Y_1(k)$, and $Y_2(k)$ of these block signals, the averaged cross spectrum $E[X^*(k)Y(k)]$ in the numerator of (4) is described by

$$E[X^*(k)Y(k)] = E[X_1^*(k)Y_1(k)] + E[X_1^*(k)Y_2(k)] + E[X_2^*(k)Y_1(k)] + E[X_2^*(k)Y_2(k)].$$

From the causality, the third term $E[X_2^*(k)Y_1(k)]$ becomes zero. Let $H_0(k)$ and $H_1(k)$ be the transfer functions from one input block to the output block signal with the same timing and the one-block delayed signal, respectively. Thus, the cross spectrum $E[X^*(k)Y(k)]$ is given by

$$E[X^*(k)Y(k)] = E[|X(k)|^2]\{H_0(k) + H_0(k) + H_1(k)\} \neq E[|X(k)|^2]\{H_0(k) + H_1(k)\}$$

that is, bias error is caused in the cross spectrum estimated in (4). From this simple example, it is found that it is significant to divide the input and output signals into short blocks and estimate the cross spectrum separately for each combination between the input blocks and the output blocks and then sum up the resultant transfer functions to obtain the total transfer function. In this section, based on the principle, a new method is proposed to decrease the bias error in $\widehat{H_{\rm all}}(k)$ of (4) and estimate an alternative transfer function $\widehat{H_{bk}}(k)$ ranging from $k = 0$ to $MN - 1$ as described below.

Let us divide the MN-point length signal into M blocks, where each of consists of N consecutive samples, as shown in Fig. 3(a). Each block is identified by the block index. When the system response is long, the transmission system in Fig. 1 is represented by a multiple input/output system as shown in Fig. 3(b). Let an indexed $H_i(k)$ be the transfer function (called the delayed block transfer function) from the input signal to the i-block-delayed-output signal, and let $h_i(n)$ be the impulse response of $H_i(k)$. The output signal $y_m(n)$ in the mth block is the sum of the responses to each input signal in the preceding blocks and the measurement noise signal $n_m(n)$ in mth block

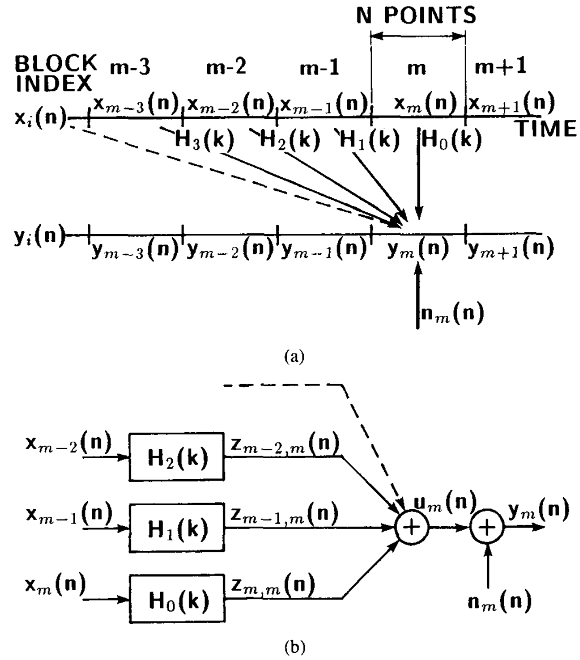

Fig. 3. When the impulse response is long, the signal transmission system model of single input/single output in Figs.1 and 3(a) is also described by the multiple input/single output transfer system as shown in Fig. 3(b).

such as

$$y_m(n) = \sum_{i=0}^{\infty} x_{m-i}(n) * h_i(n) + n_m(n) \tag{5}$$

or by its expression in the frequency domain

$$Y_m(k) = \sum_{i=0}^{\infty} H_i(k)X_{m-i}(k) + N_m(k) = \sum_{i=0}^{\infty} Z_{m-i,m}(k) + N_m(k) \tag{6}$$

where $X_m(k)$, $Y_m(k)$, and $N_m(k)$ are, respectively, the spectra of the zero-padded MN-length signals $x'_m(n)$, $y'_m(n)$, and $n'_m(n)$ of the original N-length signals $x_m(n)$, $y_m(n)$, and $n_m(n)$ in the mth block, where each is obtained as

$$x'_m(n) = \begin{cases} x_m(n), & \text{if } n = 0, 1, \ldots, N-1; \\ 0, & \text{if } n = N, N+1, \ldots, MN-1. \end{cases} \tag{7}$$

From Fig. 3(b), the spectrum $Z_{m-i,m}(k)$ of the response of $H_i(k)$ to $x_{m-i}(n)$ is defined as follows:

$$Z_{m-i,m}(k) = H_i(k)X_{m-i}(k). \tag{8}$$

The noise term $N_m(k)$ in (6) can be rewritten as

$$N_m(k) = Y_m(k) - \sum_{i=0}^{\infty} H_i(k)X_{m-i}(k).$$

The expectations of the product of $N_m(k)$ and its complex conjugate $N_m^*(k)$ give the average noise power $P_N(k)$ at the

kth frequency such as

$$\begin{aligned}P_N(k) &= E[|N_m(k)|^2] \\ &= E[|Y_m(k)|^2] - \sum_{i=0}^{\infty} H_i(k)E[X_{m-i}(k)Y_m^*(k)] \\ &\quad - \sum_{j=0}^{\infty} H_j^*(k)E[X_{m-j}^*(k)Y_m(k)] \\ &\quad + \sum_{i=0}^{\infty}\sum_{j=0}^{\infty} H_i(k)H_j^*(k)E[X_{m-i}(k)X_{m-j}^*(k)]\end{aligned}$$

where $P_N(k)$ is independent of the block index number since the signal $n(n)$ is assumed to be stationary. The least square estimate of the transfer function is obtained as that which minimizes $P_N(k)$ over all possible choice of $\{H_j(k)\}$. By setting the partial derivatives of $P_N(k)$ with respect to $\{H_j^*(k)\}$ equal to zero

$$E[X_{m-j}^*(k)Y_m(k)] = \sum_{i=0}^{\infty} H_i(k)E[X_{m-i}(k)X_{m-j}^*(k)] \quad (9)$$

where $j = 0, 1, \ldots, \infty$. Since it is assumed that the input signals $x_m(n)$ and $x_{m'}(n)$ are mutually uncorrelated for $m \neq m'$, (9) reduces to

$$E[X_{m-j}^*(k)Y_m(k)] = H_j(k)E[|X_{m-j}(k)|^2].$$

Thus

$$\widehat{H}_i(k) = \frac{E[X_{m-i}^*(k)Y_m(k)]}{E[|X_{m-i}(k)|^2]} \quad (10)$$

where $i = 0, 1, \ldots, \infty$. This gives the least square estimate of the delayed block transfer function from an input signal $x_m(n)$ in a block to the i-block delayed output signal $y_{m+i}(n)$.

A method to obtain the estimate of the total transfer system from the resultant delayed block transfer functions is described below. To begin with, let us consider the relation between the spectrum $V_i(k)$ of the ith block signal $v_i(n)$, which consists of N points in length, and the spectrum $V(k)$ of the signal $v(n)$, which consists of M blocks ($= MN$-point length), which are described as follows:

By applying the MN-point FFT to the M-block length signal

$$v(n+Ni) = v_i(n), \quad n = 0, 1, \ldots, N-1; \quad i = 0, 1, \ldots, M-1 \quad (11)$$

the resultant spectrum $V(k)$ is

$$\begin{aligned}V(k) &= \sum_{n=0}^{MN-1} v(n)\exp\left(-j2\pi\frac{kn}{MN}\right) \\ &= \sum_{i=0}^{M-1}\sum_{n=iN}^{iN+N-1} v(n)\exp\left(-j2\pi\frac{kn}{MN}\right) \\ &= \sum_{i=0}^{M-1}\sum_{n=0}^{N-1} v(n+Ni)\exp\left(-j2\pi\frac{k(n+Ni)}{MN}\right).\end{aligned}$$

Using the relation (11), $V(k)$ is

$$V(k) = \sum_{i=0}^{M-1}\left\{\sum_{n=0}^{N-1} v_i(n)\exp\left(-j2\pi\frac{kn}{MN}\right)\right\}\exp\left(-j2\pi\frac{ki}{M}\right).$$

The term in the $\{\cdot\}$ brackets of this equation is equal to the spectrum $V_i(k)$, $(k = 0, 1, \ldots, MN-1)$, which is obtained by applying the MN-point FFT to the MN-point zero-padded signal $v_i'(n)$ defined by

$$v_i'(n) = \begin{cases} v_i(n), & \text{if } n = 0, 1, \ldots, N-1; \\ 0, & \text{if } n = N, N+1, \ldots, MN-1. \end{cases} \quad (12)$$

Using the spectrum $V_i(k)$, the total spectrum $V(k)$ for the MN-point signal $v(n)$ is described by

$$V(k) = \sum_{i=0}^{M-1} V_i(k)\exp\left(-j2\pi\frac{ki}{M}\right). \quad (13)$$

In the relation of (13), by replacing $V_i(k)$ and $V(k)$, respectively, by the delayed block transfer function $\widehat{H}_i(k)$ and the total transfer function $\widehat{H_{bk}}(k)$, the estimate is given by

$$\widehat{H_{bk}}(k) = \sum_{i=0}^{M-1} \widehat{H}_i(k)\exp\left(-j2\pi\frac{ki}{M}\right). \quad (k = 0, 1, \ldots, MN-1). \quad (14)$$

Thus, the estimate $\widehat{H_{bk}}(k)$ of the total transfer function is obtained from the M spectrum estimates $\{\widehat{H}_i(k)\}$ of the delayed block transfer function in (10).

IV. Theoretical Derivations for the Transfer Function Estimates

To confirm the accuracy improvement in the estimate of $\widehat{H_{bk}}(k)$ in (14), the estimates of $\widehat{H_{\text{all}}}(k)$ in (4) and $\widehat{H_{bk}}(k)$ in (14) and their bias errors are theoretically derived in this section. To begin with, the characteristics of the true transfer function are defined in Section IV-A. Then, after deriving the theoretical expression for the expectations of the cross spectrum and power spectrum in Section IV-B, the estimates of $\widehat{H_{\text{all}}}(k)$ and $\widehat{H_{bk}}(k)$ are theoretically derived in Sections IV-C and D, respectively.

A. Definition of the Characteristics of a Transfer Function

Let us assume that the transfer system is a rational transfer function of order P and the impulse response $h(n)$ is described by

$$h(n) = \sum_{i=1}^{P} C_i p_i^n \quad (15)$$

where $\{p_i\}$ are the poles of the transfer system ($|p_i| < 1$), and $\{C_i\}$ are the complex coefficients. By defining

$$z_0 = \exp\left(-j2\pi\frac{1}{MN}\right) \quad (16)$$

the MN-point Fourier transform of the impulse response $h(n)$ is obtained by

$$\begin{aligned}H(k) &= \sum_{n=0}^{MN-1} h(n)\exp\left(-j2\pi\frac{kn}{MN}\right)\\ &= \sum_{i=1}^{P} C_i \sum_{n=0}^{MN-1} (p_i z_0^k)^n\\ &= \sum_{i=1}^{P} C_i \frac{1-(p_i z_0^k)^{MN}}{1-p_i z_0^k}. \qquad (17)\end{aligned}$$

If the length of the FFT increases to the infinite, that is, $M \to \infty$, the true transfer function $H_\infty(k)$ of $H(k)$ in (17) is given by

$$H_\infty(k) = \sum_{i=1}^{P} C_i \frac{1}{1-p_i z_0^k}. \qquad (18)$$

B. Theoretical Derivations for the Cross Spectrum

Let $F_{0m}(k;q)$ denote the kth spectrum of the signal $h(n + mN - q)$ in the mth block of the response of the transfer system to the impulse $\delta(n-q)$ at a time q in the 0th block as shown in Fig. 4(a). For the case of $m \geq 1$, by applying the MN-point FFT to the zero-padded impulse response $h'(n + mN - q)$

$$h'(n+mN-q) = \begin{cases} h(n+mN-q), & \text{if } n = 0,1,\ldots,N-1;\\ 0, & \text{if } n = N, N+1,\ldots,MN-1\end{cases}$$

and substituting (15) into the resultant spectrum, the spectrum $F_{0m}(k;q)$ is given by

$$F_{0m}(k;q) = \sum_{i=1}^{P} C_i p_i^{mN-q} \frac{1-(p_i z_0^k)^N}{1-p_i z_0^k}. \quad (\text{for } m \geq 1). \qquad (19)$$

For the case of $m = 0$, by applying the MN-point FFT to the zero-padded $(N-q)$-length impulse response $h'(n-q)$

$$h'(n-q) = \begin{cases} h(n-q), & \text{if } n = q, q+1,\ldots,N-1;\\ 0, & \text{otherwise}\end{cases}$$

the spectrum $F_{00}(k;q)$ is obtained by

$$F_{00}(k;q) = \sum_{i=1}^{P} C_i z_0^{kq} \frac{1-(p_i z_0^k)^{N-q}}{1-p_i z_0^k}, \quad (\text{for } m = 0) \qquad (20)$$

where the derivations of these spectrum $F_{0m}(k;q)$ and $F_{00}(k;q)$ in (19) and (20) are described in Appendix A.

Let $z_{0m}(n)$ $(m = 0,1,\ldots)$ denote the N-point signal in the mth block of the response of the transfer system to the input signal $x_0(n)$ in the 0th block as shown in Fig. 4(b). Using the expression for the $F_{0m}(k;q)$ of (19) and (20), the MN-point spectrum $Z_{0m}(k)$ of $z_{0m}(n)$ is obtained by

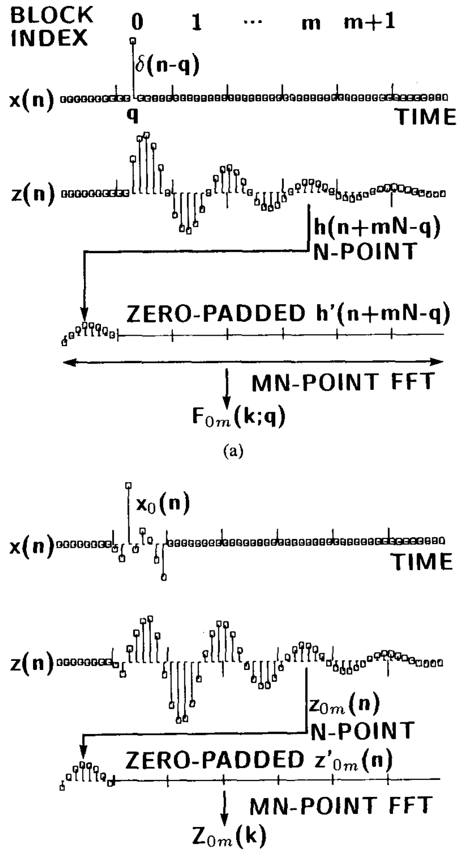

Fig. 4. (a) $F_{0m}(k;q)$denotes the MN-point spectrum of the zero-padded signal $h'(n+mN-q)$ in the mth block of the response of the transfer system to the impulse $\delta(n-q)$ at a time q in the 0th block; (b) $Z_{0m}(k)$ denotes the MN-point spectrum of the N-point signal $z_{0m}(n)$ in the mth block of the response of the transfer system to the input signal $x_0(n)$ in the 0th block.

$$Z_{0m}(k) = \sum_{q=0}^{N-1} x_0(q) F_{0m}(k;q) \qquad (21)$$

where $m = 0,1,2,\ldots$. By substituting (19) and (20) into (21)

$$\begin{aligned}Z_{0m}(k) &= \sum_{q=0}^{N-1} x_0(q) \sum_{i=1}^{P} C_i p_i^{mN-q} \frac{1-(p_i z_0^k)^N}{1-p_i z_0^k}\\ &= \sum_{i=1}^{P} C_i p_i^{mN} \frac{1-(p_i z_0^k)^N}{1-p_i z_0^k} \sum_{q=0}^{N-1} x_0(q) p_i^{-q}\\ &\qquad (m \geq 1); \qquad (22)\end{aligned}$$

$$\begin{aligned}Z_{00}(k) &= \sum_{q=0}^{N-1} x_0(q) \sum_{i=1}^{P} C_i z_0^{kq} \frac{1-(p_i z_0^k)^{N-q}}{1-p_i z_0^k}\\ &= \sum_{i=1}^{P} C_i \sum_{q=0}^{N-1} z_0^{kq} \frac{1-(p_i z_0^k)^{N-q}}{1-p_i z_0^k} x_0(q). \qquad (23)\end{aligned}$$

Letting $G_{0m}(k)$ be the expectations of the cross spectrum between $X_0(k)$ and $Z_{0m}(k)$ in (22) and (23), $G_{0m}(k)$ is given by

$$G_{0m}(k) = E[X_0^*(k)Z_{0m}(k)] = N\sigma_x^2(k)\sum_{i=1}^{P} C_i \frac{1-(p_i z_0^k)^N}{1-p_i z_0^k}\cdot\frac{1-(p_i z_0^k)^{-N}}{1-(p_i z_0^k)^{-1}} p_i^{mN}, \quad (m \geq 1) \tag{24}$$

and for the case of $m = 0$

$$G_{00}(k) = E[X_0^*(k)Z_{00}(k)] = N^2\sigma_x^2(k)\sum_{i=1}^{P} \frac{C_i}{1-p_i z_0^k}\left[1+\frac{1-(p_i z_0^k)^N}{N\{1-(p_i z_0^k)^{-1}\}}\right], \quad (m = 0) \tag{25}$$

where these derivations of the cross spectrum $G_{0m}(k)$ and $G_{00}(k)$ in (24) and (25) are described in Appendix B.

On the other hand, the expectations of the power spectrum obtained by the MN-point FFT of the zero-padded input signal $x(n)$, which consists originally of N points, is calculated by

$$E[|X(k)|^2] = E\left[\sum_{n=0}^{N-1} x_0^*(n)\exp\left(j2\pi\frac{kn}{MN}\right)\sum_{q=0}^{N-1} x_0(q)\exp\left(-j2\pi\frac{kq}{MN}\right)\right] = \sum_{n=0}^{N-1}\sum_{q=0}^{N-1} E[x_0^*(n)x_0(q)]\exp\left(-j2\pi\frac{k(q-n)}{MN}\right).$$

Since $E[x_0^*(n)x_0(q)] = \sigma_x^2\delta(n-q)$, the expectations of the power spectrum is

$$E[|X(k)|^2] = N\sigma_x^2(k)\sum_{n=0}^{N-1} 1 = N^2\sigma_x^2(k). \tag{26}$$

From the ratio of the average cross spectrum $G_{0m}(k)$ in (24) or $G_{00}(k)$ in (25) to the average power spectrum of $x(n)$ in (26), the estimates $\widehat{H_i}(k)$ in (10) for the delayed transfer function are obtained by

$$\widehat{H_i}(k) = \frac{G_{0i}(k)}{N^2\sigma_x^2(k)}, \quad \text{for i = 0, 1, 2,} \ldots \tag{27}$$

C. Transfer Function Estimates $\widehat{H_{\mathrm{all}}}(k)$ for the Standard Cross Spectrum Method

As shown previously in (4), $\widehat{H_{\mathrm{all}}}(k)$ denotes the estimate of the transfer function obtained by applying the MN-point FFT to the M-block signals $x(n)$ and $y(n)$, where each block consists of N points. The estimate $\widehat{H_{\mathrm{all}}}(k)$ is rewritten by

$$\widehat{H_{\mathrm{all}}}(k) = \frac{E[X^*(k)Y(k)]}{E[|X(k)|^2]}. \tag{4}$$

As described in Appendix C, the signals $x(n)$ and $y(n)$ are divided into M-block signals $x_i(n)$ and $y_i(n)$ ($i = 0, 1, 2, \ldots, M-1$), respectively. Using the power spectrum $|X_i(k)|^2$ and the cross spectrum $G_{l-i}(k) = E[X_i^*(k)Y_i(k)]$ of the spectrum $X_i(k)$ and $Y_i(k)$ of the resultant signals $x_i(n)$ and $y_i(n)$, the estimate $\widehat{H_{\mathrm{all}}}(k)$ in (4) is described as follows:

$$\widehat{H_{\mathrm{all}}}(k) = \sum_{m=0}^{M-1}\frac{M-m}{M}\frac{G_m(k)}{N^2\sigma_x^2(k)}\exp\left(-j2\pi\frac{km}{M}\right). \tag{28}$$

The term $G_m(k)/N^2\sigma_x^2(k)$ is equal to the $\widehat{H_m}(k)$ in (10). Thus, using the estimate $\widehat{H_m}(k)$ of the delayed block transfer function, the transfer function estimate $\widehat{H_{\mathrm{all}}}(k)$ is obtained by

$$\widehat{H_{\mathrm{all}}}(k) = \sum_{m=0}^{M-1}\frac{M-m}{M}\widehat{H_m}(k)\exp\left(-j2\pi\frac{km}{M}\right). \tag{29}$$

As described in Appendix C, by rearranging after substituting $\widehat{H_m}(k)$ in (27), the cross spectra $G_{0m}(k)$ in (24) and (25), and z_0 in (16) into (29)

$$\widehat{H_{\mathrm{all}}}(k) = \sum_{i=1}^{P} C_i\frac{1}{1-p_i z_0^k}\left[1+\frac{1}{NM}\cdot\frac{1-(p_i z_0^k)^{MN}}{1-(p_i z_0^k)^{-1}}\right]. \tag{30}$$

Since the first term $\sum_{i=1}^{P} C_i\frac{1}{1-p_i z_0^k}$ of $\widehat{H_{\mathrm{all}}}(k)$ is equal to the true transfer function $H_\infty(k)$ in (18), the remaining term shows the bias error $\Delta\widehat{H_{\mathrm{all}}}(k)$ in the estimate $\widehat{H_{\mathrm{all}}}(k)$. Thus, the bias error $\Delta\widehat{H_{\mathrm{all}}}(k)$ is given by

$$\Delta\widehat{H_{\mathrm{all}}}(k) = \widehat{H_{\mathrm{all}}}(k) - H_\infty(k) = \sum_{i=1}^{P}\frac{C_i}{1-p_i z_0^k}\cdot\frac{1}{N\{1-(p_i z_0^k)^{-1}\}}\cdot\frac{1-(p_i z_0^k)^{MN}}{M}. \tag{31}$$

D. Transfer Function Estimate $\widehat{H_{bk}}(k)$ for the Proposed Method

Let us consider the theoretical derivation for the estimate $\widehat{H_{bk}}(k)$ of the total transfer system in (14) using the definition of the impulse response $h(n)$ in (15) as follows:

By substituting $H_i(k)$ of (27) into (14) and using the definition of z_0 in (16), the estimate $\widehat{H_{bk}}(k)$ is obtained by

$$\widehat{H_{bk}}(k) = \frac{1}{N^2\sigma_x^2(k)}\left\{G_{00}(k) + \sum_{m=1}^{M-1} G_{0m}(k) z_0^{kmN}\right\}.$$

By arranging after substituting the cross spectra $G_{00}(k)$ of (24) and $G_{0m}(k)$ of (25) into this equation as described in Appendix D, the estimate $\widehat{H_{bk}}(k)$ of the total transfer system obtained by the proposed method is given by

$$\widehat{H_{bk}}(k) = \sum_{i=1}^{P}\frac{C_i}{1-p_i z_0^k}\left[1+\frac{(p_i z_0^k)^{(M-1)N}\{1-(p_i z_0^k)^N\}}{N\{1-(p_i z_0^k)^{-1}\}}\right]. \tag{32}$$

Let us consider the physical meaning of $\widehat{H_{bk}}(k)$. Let $\widehat{H_0}(k)$ be the transfer function estimate obtained by applying the standard method to the N-point input and output signals. By

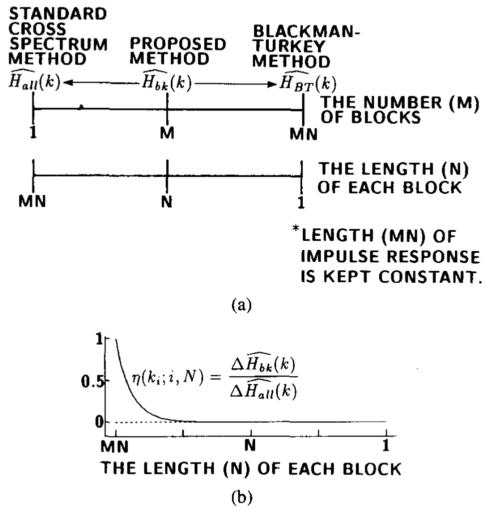

Fig. 5. (a) Relation among the proposed method, the standard cross spectrum method, and the Blackman–Tukey method; (b) theoretical ratio $\eta(k_i; i, N)$ of $\Delta\widehat{H_{bk}}(k)$ in (33) to $\Delta\widehat{H_{\rm all}}(k)$ in (31) is always equal to or less than 1 for various lengths N of each block.

substituting N into MN of the segment length in $\widehat{H_{\rm all}}(k)$ of (30), the transfer function estimate $\widehat{H_0}(k)$ is given by

$$\widehat{H_0}(k) = \sum_{i=1}^{P} C_i \frac{1}{1 - p_i z_0^k}\left[1 + \frac{1}{N}\frac{1 - (p_i z_0^k)^N}{1 - (p_i z_0^k)^{-1}}\right].$$

The second term in the right-hand side shows the bias error. In the estimate $\widehat{H_{\rm all}}(k)$ of (30), which is given when the window length N of $\widehat{H_0}(k)$ is increased to MN, the bias error of $\widehat{H_0}(k)$ is multiplied by $\frac{1}{M}\frac{1-(p_i z_0^k)^{MN}}{1-(p_i z_0^k)^N} < 1$, that is, the bias error is decreased in inverse proportion to the window length. In the estimate $\widehat{H_{bk}}(k)$ of (32), however, the bias error of $\widehat{H_0}(k)$ is multiplied by exponentially decaying term $(p_i z_0^k)^{(M-1)N} \ll 1$. Thus, a more accurate estimate of the transfer function is obtained by the proposed method.

As the same manner in (31), the first term $\sum_{i=1}^{P} C_i \frac{1}{1-p_i z_0^k}$ of $\widehat{H_{bk}}(k)$ in (32) is equal to the true transfer function $H_\infty(k)$ in (18), and the remaining term expresses the bias error $\Delta\widehat{H_{bk}}(k)$ in the estimate $\widehat{H_{bk}}(k)$. Therefore

$$\begin{aligned}\Delta\widehat{H_{bk}}(k) &= \widehat{H_{bk}}(k) - H_\infty(k)\\ &= \sum_{i=1}^{P} \frac{C_i}{1 - p_i z_0^k}\cdot\frac{1}{N\{1-(p_i z_0^k)^{-1}\}}\\ &\quad \times (p_i z_0^k)^{(M-1)N}\{1 - (p_i z_0^k)^N\}. \qquad (33)\end{aligned}$$

If the number M of the blocks and the length N of each block in (33) are substituted by 1 and MN, respectively, as shown in the extreme left of Fig. 5(a), the proposed method coincides with the standard cross spectrum method, and in this case, $\Delta\widehat{H_{bk}}(k)$ in (33) coincides exactly with $\Delta\widehat{H_{\rm all}}(k)$ in (31).

Alternatively, when the number M of the blocks and the length N of each block in (33) are substituted by MN and 1, respectively, as shown in the extreme right of Fig. 5(a), each block consists of only one point, and the number of the blocks becomes equal to the number of total points of the signals. In this case, the spectrum $Y_m(k)$ of mth block, which consists of one-point signal $y(m)$, is given by

$$\begin{aligned}\widehat{Y_m}(k) &= \sum_{n=0}^{N-1} y(n+m)\exp\left(-j2\pi\frac{kn}{MN}\right)\\ &= y(m).\end{aligned}$$

Thus, the delayed block transfer function $H_i(k)$ in (10) is obtained as

$$\begin{aligned}\widehat{H_i}(k) &= \frac{E[X_{m-i}^*(k)Y_m(k)]}{E[|X_{m-i}(k)|^2]}\\ &= \frac{E[x(m-i)^* y(m)]}{E[|x(m-i)|^2]}\\ &= \widehat{R_{xy}}(i)\end{aligned}$$

where $\widehat{R_{xy}}(i)$ denotes the estimates of the normalized correlation function between $x(n)$ and $y(n+i)$. From (14), the total transfer function, which is denoted by $\widehat{H_{BT}}(k)$, is equal to the MN-point Fourier transform of the correlation function such as

$$\begin{aligned}\widehat{H_{BT}}(k) &\stackrel{\rm def}{=} \widehat{H_{bk}}(k)\big|_{M\leftarrow MN, N\leftarrow 1}\\ &= \sum_{i=0}^{MN-1} \widehat{R_{xy}}(i)\exp\left(-j2\pi\frac{ki}{MN}\right) \qquad (34)\end{aligned}$$

which corresponds to the spectrum estimates obtained by the Blackman–Tukey(B-T) method [19]. By substituting MN and 1 into M and N of (33), respectively, the bias error $\Delta\widehat{H_{BT}}(k)$ in the estimate $\widehat{H_{BT}}(k)$ is given by

$$\begin{aligned}\Delta\widehat{H_{BT}}(k) &= \Delta\widehat{H_{bk}}(k)\Big|_{M\leftarrow MN, N\leftarrow 1}\\ &= \sum_{i=1}^{P} C_i \cdot \frac{1}{\{1-(p_i z_0^k)^{-1}\}}\cdot(p_i z_0^k)^{MN-1}. \qquad (35)\end{aligned}$$

V. Accuracy Comparison Based on the Theoretically Derived Equations

By comparing the difference of the bias error between $\Delta\widehat{H_{\rm all}}(k)$ in (31) and $\Delta\widehat{H_{bk}}(k)$ in (33), it is clear that there is difference between them only in the third terms $(p_i z_0^k)^{(M-1)N}\{1 - (p_i z_0^k)^N\}$ in $\Delta\widehat{H_{bk}}(k)$ and $\frac{1}{M}\{1 - (p_i z_0^k)^{MN}\}$ in $\Delta\widehat{H_{\rm all}}(k)$. When the actual length of the signal involved in the zero-padded signal is equal to N, let us define the ratio $\eta(k; i, N)$ of $\Delta\widehat{H_{bk}}(k)$ to $\Delta\widehat{H_{\rm all}}(k)$ for each order i of the impulse response $C_i p_i^n$ of the poles in the transfer system as follows:

$$\begin{aligned}\eta(k; i, N) &\stackrel{\rm def}{=} \frac{\Delta\widehat{H_{bk}}(k)}{\Delta\widehat{H_{\rm all}}(k)}\\ &= M(p_i z_0^k)^{(M-1)N}\frac{1-(p_i z_0^k)^N}{1-(p_i z_0^k)^{MN}}\\ &= \frac{MN(p_i z_0^k)^{MN}}{1-(p_i z_0^k)^{MN}}\times\frac{(p_i z_0^k)^{-N} - 1}{N}. \qquad (36)\end{aligned}$$

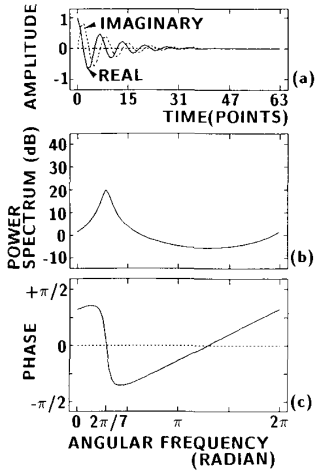

Fig. 6. (a) Examples of the impulse response $h(n)$ in (15) employed in Figs. 7 and 8; (b), (c) frequency characteristics $H_\infty(k)$ of the signal in Fig. 6(a) defined by (18). The order P of the rational transfer function is equal to 1, $C_1 = 1, |p_1| = 0.90$, and $\angle p_1 = \frac{2\pi}{7}$. The length MN is equal to 64.

The first term $\frac{MN(p_i z_0^k)^{MN}}{1-(p_i z_0^k)^{MN}}$, which we denote by $D(k;i)$ hereafter, depends not on N but on the total length MN of the impulse response, which is assumed to be a constant value.

Since the bias error is large especially around the resonant frequency, let us evaluate $\eta(k;i,N)$ at and near the resonant frequency as follows: At the resonant frequency $k_i = MN\angle p_i/2\pi$ of the ith pole, the complex term $p_i z_0^k$ becomes a real value, which we denote by a $(0 < a < 1)$. Thus, the ratio $\eta(k;i,N)$ and $D(k;i)$ become real at $k = k_i$. In this case, the ratio $\eta(k_i;i,N)$ at $k = k_i$ is given by

$$\eta(k_i;i,N) = D(k_i;i)\frac{a^{-N}-1}{N} \tag{37}$$

where $D(k;i) > 0$. Since the partial derivation of $a^{-N} = \exp(-N\ln a)$ with respect to N is equal to $-a^{-N}\ln a$, the partial derivation of $\eta(k_i;i,N)$ with respect to N is given by

$$\frac{\partial\eta(k_i;i,N)}{\partial N} = D(k_i;i)\left\{-\frac{a^{-N}-1}{N^2} - \frac{a^{-N}\ln a}{N}\right\} = \frac{D(k_i;i)a^{-N}}{N^2}(a^N - \ln a^N - 1).$$

Since the second term $(a^N - \ln a^N - 1)$ is positive for $0 < a^N < 1$, the gradient $\frac{\partial\eta(k_i;i,N)}{\partial N}$ of $\eta(k_i;i,N)$ is positive for $0 < a^N < 1$. Thus, $\eta(k_i;i,N)$ increases monotonically as N becomes larger in the range of $1 \le N \le MN$ as illustrated in Fig. 5(b). When N is equal to MN, that is, $M = 1$, $\Delta\widehat{H_{bk}}(k)$ becomes equal to $\Delta\widehat{H_{\rm all}}(k)$ as described previously. In this case, $\eta(k;i,N = MN) = 1$. Therefore, the bias error $\Delta\widehat{H_{bk}}(k)$ in the proposed method is always less than or equal to $\Delta\widehat{H_{\rm all}}(k)$ in the standard cross spectrum method at the resonant frequency, that is

$$\Delta\widehat{H_{\rm all}}(k) \ge \Delta\widehat{H_{bk}}(k) \ge \Delta\widehat{H_{BT}}(k). \tag{38}$$

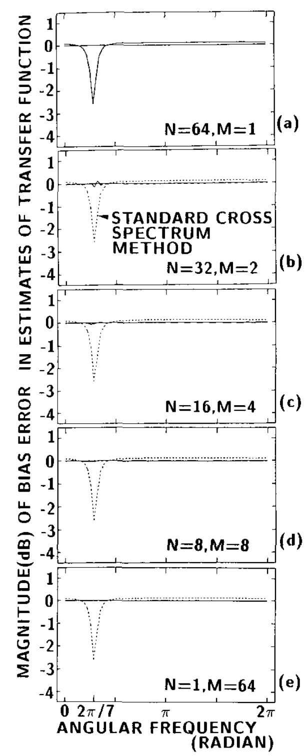

Fig. 7. Magnitude characteristics of the bias error in the estimate $\widehat{H_{bk}}(k)$ by the proposed method in (32) for different five combinations of the number M of the blocks and the length N of a block. The dotted line shows the bias error $\Delta\widehat{H_{\rm all}}(k)$ in the estimate $\widehat{H_{\rm all}}(k)$ of the standard cross spectrum method in (30): (a) $N = 64, M = 1$; (b) $N = 32, M = 2$; (c) $N = 16, M = 4$; (d) $N = 8, M = 8$; (e) $N = 1, M = 64$.

Fig. 6 shows an example of the impulse response $h(n)$ in (15) and its frequency characteristics $H_\infty(k)$ in (18) for the case where the order P of the rational transfer function is equal to 1, $C_1 = 1$, $|p_1| = 0.90$, and $\angle p_1 = \frac{2\pi}{7}$. The length MN is equal to 64.

Figs. 7 and 8 show, respectively, the magnitude and phase characteristics of the bias error $\Delta\widehat{H_{bk}}(k)$ of the proposed method in (33) for five different combinations of M and N under the condition that the total length MN is always equal to 64. The dotted line shows the bias error $\Delta\widehat{H_{\rm all}}(k)$ of the standard cross spectrum method in (31). The bias error in $\widehat{H_{\rm all}}(k)$ is large especially at and near the resonant frequency $k_1 = \frac{\angle p_1}{2\pi} \times MN$.

In Figs. 7(a) and 8(a), the bias error of $\widehat{H_{bk}}(k)$ coincides with that of $\widehat{H_{\rm all}}(k)$ because the number M of the block is equal to 1 in these figures. As the number M of the blocks is increased from top to bottom in Figs. 7 and 8, the estimation accuracy is remarkably improved.

Figs. 9 and 10 show the characteristics of the bias error $\Delta\widehat{H_{bk}}(k)$ as a function of the value of M, where the total length MN is 64 and $\angle p_1 = \frac{2\pi}{7}$. The magnitude in Fig. 9 and the phase in Fig. 10 of the bias error are represented by the values at the discrete frequency $k_1 = \frac{\angle p_1}{2\pi} \times MN \simeq 9$ and $k_1 = 10$, respectively. The dotted line shows the bias

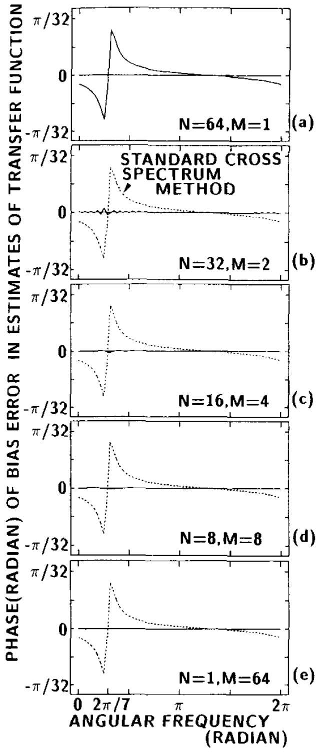

Fig. 8. Phase characteristics of the bias error in the estimate $\widehat{H_{bk}}(k)$ by the proposed method in (32) for different five combinations of the number M of the blocks and the length N of a block. The dotted line shows the bias error $\Delta\widehat{H_{\rm all}}(k)$ in the estimate $\widehat{H_{\rm all}}(k)$ of the standard cross spectrum method in (30): (a) $N = 64, M = 1$; (b) $N = 32, M = 2$; (c) $N = 16, M = 4$; (d) $N = 8, M = 8$; (e) $N = 1, M = 64$.

error in the estimate $\widehat{H_{\rm all}}(k)$ of the standard cross spectrum method. For three different values of the magnitude of p_1 ($|p_1| = 0.95$, $|p_1| = 0.9$, and $|p_1| = 0.5$), the results are shown in Figs. 9(a) and 10(a), Figs. 9(b) and 10(b), and Figs. 9(c) and 10(c), respectively. It is obvious that the bias error decreases as the number M of the blocks becomes large. For the case of $M \geq 2$, the bias error of the proposed method is significantly less than that of the standard cross spectrum method, and the resultant bias error $\Delta\widehat{H_{bk}}(k)$ of the proposed method is small enough for the accurate estimation of the transfer function.

VI. Computer Simulation Experiments

In order to illustrate the advantage of the proposed method to estimate the transfer function $H(k)$ or its impulse response $h(n)$, we choose the example of the fourth order all-pole transfer model $H_\infty(k)$, where poles are $0.996\exp(\pm 2\pi \cdot 65/360)$ and $0.997\exp(\pm 2\pi \cdot 80/360)$ as shown in Fig. 11(1-b). The input signal $x(n)$ in (1) is assumed to be white noise, and the output signal $y(n)$ is contaminated by measured white noise $n(n)$, which is uncorrelated with the driving series $x(n)$. The SNR equals 15 dB, and 32 768 points are generated for each of the signals $x(n)$ and $y(n)$. The generated two signals $x(n)$ and $y(n)$ are then divided into 128 sections, each of which has length (MN) equal to 256 points. The true impulse response $h_\infty(n)$ of $H_\infty(k)$ is shown for the same length in Fig. 11(1-a). Assuming that the true length of the impulse response is not known *a a priori*, the impulse response is estimated for the length $MN = 256$ points in the following experiments for both the standard method and for the proposed method.

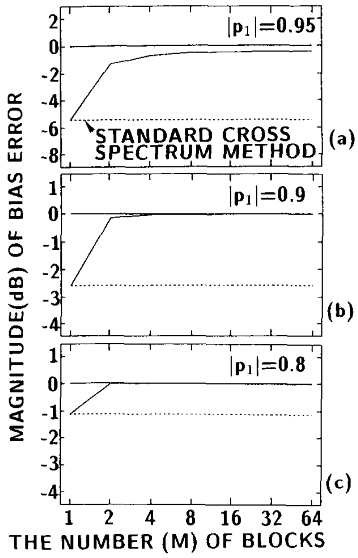

Fig. 9. Relation between the number M of blocks used in the proposed method and the magnitude of the bias error $\Delta\widehat{H_{bk}}(k)$ in (33) at the resonant frequency $k_1 = \frac{\angle p_1}{2\pi} \times MN \simeq 9$ under the condition that the total length MN is always equal to 64. $\angle p_1 = \frac{2\pi}{7}$. The dotted line shows the bias error in the estimate $\widehat{H_{\rm all}}(k)$ of the standard cross spectrum method: (a) $|p_1| = 0.95$; (b) $|p_1| = 0.9$; (c) $|p_1| = 0.8$.

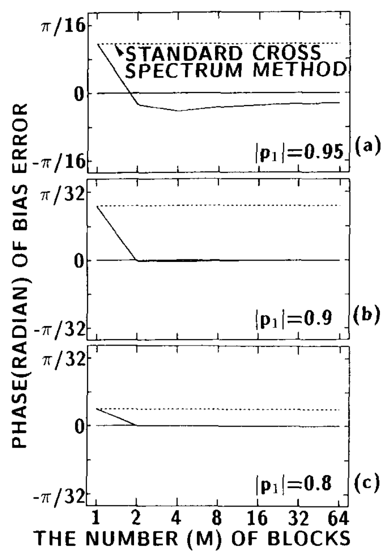

Fig. 10. Relation between the number M of blocks used in the proposed method and the phase of the bias error $\Delta\widehat{H_{bk}}(k)$ in (33) near the resonant frequency $k_1 = 10$ under the condition that the total signal length MN is always equal to 64. $\angle p_1 = \frac{2\pi}{7}$. The dotted line shows the bias error in the estimate $\widehat{H_{\rm all}}(k)$ of the standard cross spectrum method: (a) $|p_1| = 0.95$; (b) $|p_1| = 0.9$; (c) $|p_1| = 0.8$.

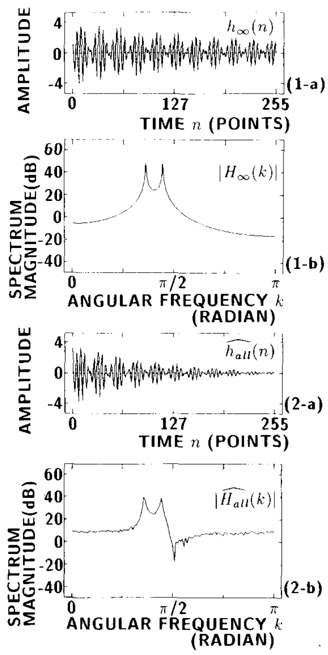

Fig. 11. (1) Magnitude characteristics of the fourth-order all-pole transfer model $H_\infty(k)$ employed in the computer simulation in Section VI and its impulse response $h_\infty(n)$; (2) transfer function estimate $\widehat{H_{\rm all}}(k)$ and its impulse response $\widehat{h_{\rm all}}(k)$ obtained by the standard method described in Section II.

Fig. 11(2) shows the transfer function estimates $\widehat{H_{\rm all}}(k)$ and the impulse response estimate $\widehat{h_{\rm all}}(n)$, which are obtained by applying the standard method in Section II to the signals $x(n)$ and $y(n)$ in each segment with length $MN = 256$, which is divided above. The number of the nonoverlapping average operation $E[\cdot]$ in (4) is equal to 128 times. As described previously in Section II, the estimate $\widehat{H_{\rm all}}(k)$ is obtained so that the impulse response to every input impulse in a segment is truncated at the end of the segment. In the magnitude of the transfer function estimate $\widehat{H_{\rm all}}(k)$ in Fig. 11(2-b), a spectrum zero appears due to the truncation. The resultant impulse response estimate $\widehat{h_{\rm all}}(n)$ in Fig. 11(2-a) converges more rapidly than the true characteristic $h_\infty(n)$ in Fig. 11(1-a). From these results, the true length of the impulse response $h_\infty(n)$ cannot be estimated by the standard method.

Figs. 12 and 14 show the results obtained by the method proposed in Section III. For the results in Figs. 12 and 14(1), each segment with length $MN = 128$ is divided into nonoverlapping 8 blocks, each of which has 32 points in length, that is, in (7), (10), and (14), the number M of the blocks and the length N of each block are 8 and 32, respectively. Fig 12 shows the impulse response estimates $\widehat{h_i}(n), (i = 0, 1, 2, \ldots, 8)$, which are obtained from the discrete Fourier transform (DFT) of $\widehat{H_i}(k) \cdot \exp(-j2\pi \cdot ki/M)$ in the right-hand side of (14). The impulse response $\widehat{h_i}(n)$ shows the transfer characteristics from the zero-padded input signal $x'_m(n)$ in the mth block with length N to the zero-padded i-block delayed output signal $y'_{m+i}(n)$. For the estimate $\widehat{h_0}(n)$ in Fig. 12(a),

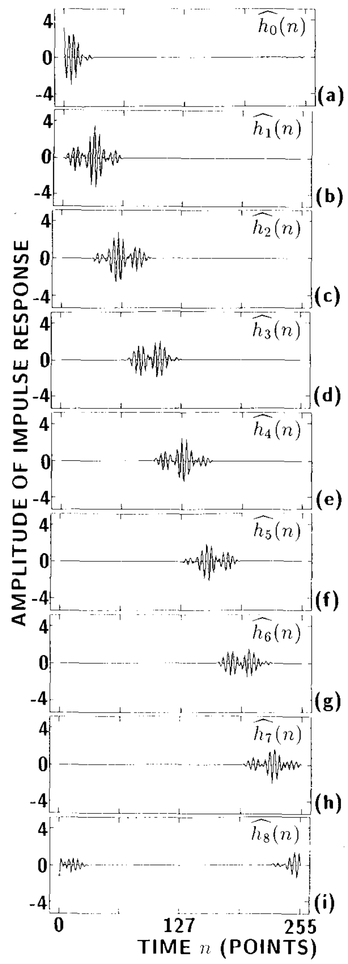

Fig. 12. Impulse response estimates $\widehat{h_i}(n)$, $(i = 0, 1, \ldots, 8)$, which are obtained by applying DFT to the block transfer function estimates $\widehat{H_i}(k)$ multiplied by shift coefficients $\exp(-j2\pi \cdot ki/M)$. In the proposed method in Section III, each segment with length $MN = 128$ is divided into nonoverlapping 8 blocks, where each has 32 points in length ($M = 8$, $N = 32$).

the lengths ℓ of the shortest and longest paths from the input block to the output block are 0 and $N - 1$, respectively, as shown in Fig. 13(a). However, for $\widehat{h_1}(n)$ in Fig. 12(b), the lengths ℓ of the shortest and longest paths are 1 and $2N - 1$, respectively, as shown in Fig. 13(b). Thus, the duration time of the resultant impulse response estimate is $2N-1$ for $\widehat{h_1}(n)$, $\widehat{h_2}(n), \ldots, \widehat{h_8}(n)$ as shown in Figs. 12(b)-(i). For the estimates $\widehat{h_8}(n)$ in Fig. 12(i), the later half of the estimates is shifted to the beginning of the estimates due to the aliasing in the above DFT operation of $\widehat{H_i}(k) \cdot \exp(-j2\pi \cdot ki/M)$.

Thus, by eliminating the beginning part of the estimate $\widehat{h_8}(n)$ and summing up the resultant estimates $\widehat{H_i}(k) \cdot \exp(-j2\pi \cdot ki/M)$ for $i = 0, 1, \ldots, 8$ in (14), the transfer function estimates $\widehat{H_{bk}}(k)$, and its impulse response $\widehat{h_{bk}}(n)$ is obtained as shown in Figs. 14(1-b) and (1-c), respectively. The impulse response estimates $\widehat{h_{bk}}(n)$ in Fig. 14(1-a) almost

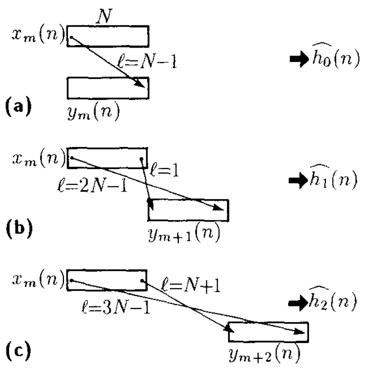

Fig. 13. Illustrations for explaining the relations between the length ℓ of the estimated impulse response in Fig. 12 for each block transfer function and the amount of time for which the output block is delayed from the input block.

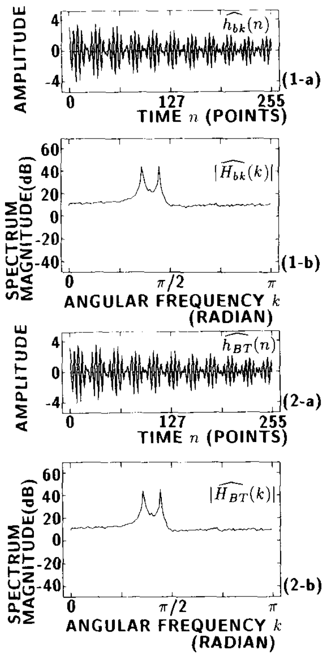

Fig. 14. (1) Transfer function estimate $\widehat{H_{bk}}(k)$ and its impulse response $\widehat{h_{\rm all}}(k)$ obtained by the proposed method described in Section III ($M = 8$, $N = 32$); (2) transfer function estimate $\widehat{H_{BT}}(k)$ and its impulse response $\widehat{h_{BT}}(k)$ obtained by the proposed method described in Section IV-D ($M = 128$, $N = 1$).

coincide with the true characteristics $H_\infty(k)$ in Fig. 11(1-a) except for the amplitude $\widehat{h_{bk}}(0)$ for the first point, which is affected by the contaminated noise components. For the same reason, the magnitude of the transfer function $\widehat{H_{bk}}(k)$ in Fig. 14(1-b) has bias error, especially for the base part of its resonant characteristics. These errors will decrease with an increase in the average number. From these figures, the estimates obtained by the standard method are improved by the proposed method.

Fig. 14(2) shows the estimates $\widehat{H_{BT}}(k)$ in (34) and its impulse response $\widehat{h_{bk}}(n)$, where each segment with length MN is divided into MN blocks, where each has one point in length. These results almost coincide with those in Fig. 14(1).

VII. Concluding Remarks

This paper proposes a new method that accurately estimates the transfer function of a transfer system with a long impulse response. To begin with, a delayed block transfer function was introduced to detect components that are correlated to the signal in the input window but leaks from the output window. The delayed block transfer function is defined as the transfer function that is calculated by use of the input signal and the output signal in the *a delayed* output window. Next, from the resultant delayed block transfer functions, the total transfer function is estimated, and the estimation accuracy is improved by the proposed method.

We have also described the derivation of the thorough theoretical expressions for the estimates of the transfer functions obtained by the proposed and standard methods. By comparing these expressions, the accuracy and the usefulness of the proposed method was confirmed. From the computer simulation experiments, the advantage of the proposed method was also confirmed.

Two issues remain for further research as follows: In the theoretical derivations and the simulation experiments, the block transfer functions are computed over contiguous *nonoverlapping* blocks of the input and output signals, where each block is cut off from the signals by using a *a rectangular window*. As described in Section I, however, considerable work has been done by Carter and Nuttall [37], [41] in applying Welch's approach [5] to the estimation of the spectra and cross spectra when the data blocks are overlapping. Moreover, it is also necessary to determine the optimum window applied to each block when it is cut off from the original signal. These important issues are currently under investigation. It is also important to apply the proposed method to some practical examples.

Appendix A

Derivations for the Spectrum $F_{0m}(k;q)$ in Section IV-B

The kth spectrum $F_{0m}(k;q)$ of the signal $h(n+mN-q)$ in the mth block of the response of the transfer system to the impulse $\delta(n-q)$ at a time q in the 0th block as shown in Fig. 4(a) is obtained as follows: For the case of $m \geq 1$, by applying the MN-point FFT to the zero-padded impulse response $h'(n+mN-q)$ defined by

$$h'(n+mN-q) = \begin{cases} h(n+mN-q), & \text{if } n = 0, 1, \ldots, N-1; \\ 0, & \text{if } n = N, N+1, \ldots, MN-1 \end{cases}$$

the spectrum $F_{0m}(k;q)$ is given by

$$F_{0m}(k;q) = \sum_{n=0}^{N-1} h(n+mN-q) z_0^{kn}, \quad (\text{for } m \geq 1) \quad (\text{A.1})$$

where $z_0 = \exp(-j2\pi/MN)$ as defined in (16). For the case of $m = 0$, by applying the MN-point FFT to the zero-padded

$(N-q)$-length impulse response $h'(n-q)$

$$h'(n-q) = \begin{cases} h(n-q), & \text{if } n = q, q+1, \ldots, N-1; \\ 0, & \text{otherwise} \end{cases}$$

the spectrum $F_{00}(k;q)$ is obtained by

$$F_{00}(k;q) = \sum_{n=q}^{N-1} h(n-q) z_0^{kn}. \tag{A.2}$$

By substituting $h(n)$ defined in (15) into (A.1) and (A.2), the spectra $F_{0m}(k;q)$ and $F_{00}(k;q)$ are, respectively, described by

$$\begin{aligned} F_{0m}(k;q) &= \sum_{n=0}^{N-1} \sum_{i=1}^{P} C_i p_i^{n+mN-q} z_0^{kn} \\ &= \sum_{i=1}^{P} C_i p_i^{mN-q} \sum_{n=0}^{N-1} (p_i z_0^k)^n \\ &= \sum_{i=1}^{P} C_i p_i^{mN-q} \frac{1-(p_i z_0^k)^N}{1-p_i z_0^k} \\ &\quad (m \geq 1); \end{aligned} \tag{A.3}$$

$$\begin{aligned} F_{00}(k;q) &= \sum_{n=q}^{N-1} \sum_{i=1}^{P} C_i p_i^{n-q} z_0^{kn} \\ &= \sum_{i=1}^{P} C_i z_0^{kq} \sum_{n=0}^{N-q-1} (p_i z_0^k)^n \\ &= \sum_{i=1}^{P} C_i z_0^{kq} \frac{1-(p_i z_0^k)^{N-q}}{1-p_i z_0^k}. \end{aligned} \tag{A.4}$$

Equations (A.3) and (A.4) are used in (19) and (20), respectively, in the text.

Appendix B

Derivations for the Cross Spectrum $G_{0m}(k)$ in Section IV-B

The expectations $G_{0m}(k)$ of the cross spectrum between the spectrum $X_0(k)$ of the input signal in the 0th block and the spectrum $Z_{0m}(k)$ of the N-point signal in the mth block of the response of the transfer system to the $x_0(n)$ in (22) and (23) is given by

$$\begin{aligned} &G_{0m}(k) \\ &= E[X_0^*(k) Z_{0m}(k)] \\ &= E\left[\sum_{n=0}^{N-1} x_0^*(n) z_0^{-kn} \sum_{i=1}^{P} C_i p_i^{mN} \frac{1-(p_i z_0^k)^N}{1-p_i z_0^k} \sum_{q=0}^{N-1} x_0(q) p_i^{-q}\right] \\ &= \sum_{i=1}^{P} C_i p_i^{mN} \frac{1-(p_i z_0^k)^N}{1-p_i z_0^k} \sum_{n=0}^{N-1} \sum_{q=0}^{N-1} E[x_0^*(n) x_0(q)] z_0^{-kn} p_i^{-q} \end{aligned} \tag{B.1}$$

for the case of $m \geq 1$. Since the variance of the input signal $x(n)$ is assumed to be σ_x^2 as described in Section II,

$$E[x_0^*(n) x_0(q)] = \sigma_x^2 \delta(n-q)$$

where

$$\delta(n) = \begin{cases} 1, & \text{if } n = 0; \\ 0, & \text{otherwise.} \end{cases}$$

Letting each spectrum component of $X(k)$ have the power

$$\sigma_x^2(k) = \frac{\sigma_x^2}{N} \tag{B.2}$$

at the kth frequency

$$\begin{aligned} G_{0m}(k) &= \sum_{i=1}^{P} C_i p_i^{mN} \frac{1-(p_i z_0^k)^N}{1-p_i z_0^k} N \sigma_x^2(k) \sum_{n=0}^{N-1} z_0^{-kn} p_i^{-n} \\ &= N\sigma_x^2(k) \sum_{i=1}^{P} C_i \frac{1-(p_i z_0^k)^N}{1-p_i z_0^k} \cdot \frac{1-(p_i z_0^k)^{-N}}{1-(p_i z_0^k)^{-1}} p_i^{mN}. \end{aligned} \tag{B.3}$$

For the case of $m = 0$, using (23), the cross spectrum $G_{00}(k)$ is given by

$$\begin{aligned} &G_{00}(k) \\ &= E[X_0^*(k) Z_{00}(k)] \\ &= E\left[\sum_{n=0}^{N-1} x_0^*(n) z_0^{-kn} \sum_{i=1}^{P} C_i \sum_{q=0}^{N-1} z_0^{kq} \frac{1-(p_i z_0^k)^{N-q}}{1-p_i z_0^k} x_0(q)\right] \\ &= \sum_{i=1}^{P} C_i \sum_{n=0}^{N-1} \sum_{q=0}^{N-1} E[x_0^*(n) x_0(q)] z_0^{-kn} z_0^{kq} \frac{1-(p_i z_0^k)^{N-q}}{1-p_i z_0^k} \\ &= \sum_{i=1}^{P} C_i N \sigma_x^2(k) \frac{1}{1-p_i z_0^k} \sum_{n=0}^{N-1} \{1-(p_i z_0^k)^{N-n}\} \\ &= N\sigma_x^2(k) \sum_{i=1}^{P} \frac{C_i}{1-p_i z_0^k} \left[N - \frac{(p_i z_0^k)^N \{1-(p_i z_0^k)^{-N}\}}{1-(p_i z_0^k)^{-1}}\right] \\ &= N^2 \sigma_x^2(k) \sum_{i=1}^{P} \frac{C_i}{1-p_i z_0^k} \left[1 + \frac{1-(p_i z_0^k)^N}{N\{1-(p_i z_0^k)^{-1}\}}\right]. \end{aligned} \tag{B.4}$$

Equations (B.3) and (B.4) are used in (24) and (25), respectively, in the text.

Appendix C

Derivations for the Transfer Function Estimates $\widehat{H_{\rm all}}(k)$ for the Standard Cross Spectrum Method in Section IV-C

As shown in (4), $\widehat{H_{\rm all}}(k)$ denotes the estimate of the transfer function obtained by applying the MN-point FFT to the M-block signals $x(n)$ and $y(n)$, where each block consists of N points. The estimate $\widehat{H_{\rm all}}(k)$ is rewritten by

$$\widehat{H_{\rm all}}(k) = \frac{E[X^*(k)Y(k)]}{E[|X(k)|^2]} \tag{4}$$

where MN-point length signals $X(k)$ and $Y(k)$ are obtained from (13) by

$$\begin{aligned} X(k) &= \sum_{i=0}^{M-1} X_i(k) \exp\left(-j2\pi \frac{ki}{M}\right), \\ Y(k) &= \sum_{i=0}^{M-1} Y_i(k) \exp\left(-j2\pi \frac{ki}{M}\right) \end{aligned} \tag{C.1}$$

and $X_i(k)$ and $Y_i(k)$ are spectra obtained by applying the MN-point FFT to the zero-padded MN-point signals $x_i'(n)$ and $y_i'(n)$, respectively, as defined in (12). Since the signals $\{x_i(n)\}$ are mutually uncorrelated, the denominator of (4) is calculated from (C.1) such as

$$\begin{aligned}
&E[|X(k)|^2] \\
&= E\left[\left\{\sum_{i=0}^{M-1} X_i^*(k)e^{j2\pi ki/M}\right\}\left\{\sum_{l=0}^{M-1} X_l(k)e^{-j2\pi kl/M}\right\}\right] \\
&= \sum_{i=0}^{M-1} E[|X_i(k)|^2] \\
&= MN^2\sigma_x^2(k) \qquad \text{(C.2)}
\end{aligned}$$

where the definition of $E[|X(k)|^2]$ is different from that of $E[|X(k)|^2]$ in (26).

On the other hand, the numerator of (4) is written by

$$\begin{aligned}
&E[X^*(k)Y(k)] \\
&= E\left[\left\{\sum_{i=0}^{M-1} X_i^*(k)e^{j2\pi ki/M}\right\}\left\{\sum_{l=0}^{M-1} Y_l(k)e^{-j2\pi kl/M}\right\}\right] \\
&= \sum_{i=0}^{M-1}\sum_{l=0}^{M-1} E[X_i^*(k)Y_l(k)]\exp\left(-j2\pi\frac{k(l-i)}{M}\right). \qquad \text{(C.3)}
\end{aligned}$$

Using the causality of the transfer system

$$E[X_i^*(k)Y_l(k)] = 0 \text{ for } i > l. \qquad \text{(C.4)}$$

Since the input and output signals are assumed to be stationary, the cross spectrum $G_{l-i}(k) = E[X_i^*(k)Y_l(k)]$ between $X_i(k)$ and $Y_l(k)$ in the right-hand side of (C.3) is given by

$$\begin{aligned}
G_{l-i}(k) &= E[X_i^*(k)Y_l(k)] \\
&= E[X_0^*(k)Y_{l-i}(k)]. \qquad \text{for } l \geq i. \qquad \text{(C.5)}
\end{aligned}$$

Thus, the numerator of (4) is obtained by

$$\begin{aligned}
E[X^*(k)Y(k)] &= \sum_{i=0}^{M-1}\sum_{l=i}^{M-1} G_{l-i}(k)\exp\left(-j2\pi\frac{k(l-i)}{M}\right) \\
&= \sum_{i=0}^{M-1}\sum_{m=0}^{M-1-i} G_m(k)\exp\left(-j2\pi\frac{km}{M}\right) \\
&= \sum_{m=0}^{M-1}(M-m)G_m(k)\exp\left(-j2\pi\frac{km}{M}\right). \qquad \text{(C.6)}
\end{aligned}$$

By substituting (C.2) and (C.3) into (4)

$$\widehat{H_{\mathrm{all}}}(k) = \sum_{m=0}^{M-1}\frac{M-m}{M}\frac{G_m(k)}{N^2\sigma_x^2(k)}\exp\left(-j2\pi\frac{km}{M}\right). \qquad \text{(C.7)}$$

The term $G_m(k)/N^2\sigma_x^2(k)$ is equal to the $\widehat{H_m}(k)$ in (10). Thus, using the estimate $\widehat{H_i}(k)$ of the delayed block transfer function, the transfer function estimate $\widehat{H_{\mathrm{all}}}(k)$ is obtained by

$$\widehat{H_{\mathrm{all}}}(k) = \sum_{m=0}^{M-1}\frac{M-m}{M}\widehat{H_m}(k)\exp\left(-j2\pi\frac{km}{M}\right). \qquad \text{(C.8)}$$

By rearranging after substituting $\widehat{H_m}(k)$ in (27) and z_0 in (16) into (C.8)

$$\begin{aligned}
\widehat{H_{\mathrm{all}}}(k) &= \frac{1}{N^2\sigma_x^2(k)}\left\{G_{00}(k) + \sum_{m=1}^{M-1}\frac{M-m}{M}G_{0m}(k)z_0^{kmN}\right\} \\
&= \frac{1}{N}\sum_{i=1}^{P} C_i\frac{1}{1-r^k} \times \left[N + \frac{1-r^N}{1-r^{-1}}\right. \\
&\quad \left. + \frac{(1-r^N)(1-r^{-N})}{1-r^{-1}}\sum_{m=1}^{M-1}\frac{M-m}{M}r^{mN}\right] \qquad \text{(C.9)}
\end{aligned}$$

where the cross spectra $G_{0m}(k)$ in (24) and $G_{00}(k)$ in (25) are used, and r is defined by $p_i z_0^k$. Using the relation $\sum_{n=1}^{K} nx^n = \frac{x(1-x^K)}{(1-x)^2} - \frac{Kx^{K+1}}{1-x}$, the last term $\sum_{m=1}^{M-1}\frac{M-m}{M}r^{mN}$ of (C.9) is rearranged as follows:

$$\begin{aligned}
&\sum_{m=1}^{M-1}\frac{M-m}{M}r^{mN} \\
&= r^N\sum_{m=0}^{M-2} r^{mN} - \frac{1}{M}\sum_{m=1}^{M-1} mr^{mN} \\
&= r^N\frac{1-r^{(M-1)N}}{1-r^N} \\
&\quad - \frac{1}{M}\left\{\frac{r^N(1-r^{(M-1)N})}{(1-r^N)^2} - \frac{(M-1)r^{MN}}{1-r^N}\right\} \\
&= \frac{r^N}{M(1-r^N)^2}\left\{M(1-r^{(M-1)N})(1-r^N)\right. \\
&\quad \left. - (1-r^{(M-1)N}) + (M-1)(1-r^N)r^{(M-1)N}\right\} \\
&= \frac{r^N}{M(1-r^N)^2}\left\{(M-1) - Mr^N + r^{MN}\right\}. \qquad \text{(C.10)}
\end{aligned}$$

Using this result, the term in the square brackets $[\cdot]$ in (C.9) is rewritten as follows:

$$\begin{aligned}
[\cdot] = N + \frac{1}{M(1-r^{-1})(1-r^N)}&\left\{M(1-r^N)^2\right. \\
&\left. + r^N(1-r^{-N})(M-1-Mr^N+r^{NM})\right\}. \qquad \text{(C.11)}
\end{aligned}$$

Since the term in the braces $\{\cdot\}$ of (C.11) is equal to $(1 - r^N)(1-r^{NM})$, the term $[\cdot]$ in (C.9) or (C.11) is rearranged as

$$[\cdot] = N + \frac{(1-r^{NM})}{M(1-r^{-1})}. \qquad \text{(C.12)}$$

Thus, the theoretical expression of $\widehat{H_{\text{all}}}(k)$ is summarized as follows:

$$\begin{aligned}\widehat{H_{\text{all}}}(k) &= \frac{E[X^*(k)Y(k)]}{E[|X(k)|^2]} \\ &= \frac{\sum_{i=0}^{M-1}\sum_{l=0}^{M-1} E[X_i^*(k)Y_l(k)]\exp\left(-j2\pi\frac{k(l-i)}{M}\right)}{E[|X(k)|^2]} \\ &= \sum_{m=0}^{M-1}\frac{M-m}{M}\widehat{H}_m(k)\exp\left(-j2\pi\frac{km}{M}\right) \\ &= \sum_{i=1}^{P} C_i\frac{1}{1-p_iz_0^k}\left[1+\frac{1}{NM}\cdot\frac{1-(p_iz_0^k)^{MN}}{1-(p_iz_0^k)^{-1}}\right]. \quad (C.13)\end{aligned}$$

This expression is used in (30) of the text.

APPENDIX D

Derivations of the Transfer Function Estimate $\widehat{H_{bk}}(k)$ *for the Proposed Method in Section IV-D*

In this Appendix, the theoretical derivation for the estimate $\widehat{H_{bk}}(k)$ of the total transfer system in (14) is derived using the definition of the impulse response in (15) as follows:

By substituting the estimates $\widehat{H_i}(k)$ of (27) into (14) and using the definition of z_0 in (16), the estimate $\widehat{H_{bk}}(k)$ is obtained by

$$\widehat{H_{bk}}(k) = \frac{1}{N^2\sigma_x^2(k)}\left\{G_{00}(k)+\sum_{m=1}^{M-1}G_{0m}(k)z_0^{kmN}\right\}. \quad (D.1)$$

Substituting the cross spectra $G_{00}(k)$ of (24) and $G_{0m}(k)$ of (25) into this equation

$$\begin{aligned}\widehat{H_{bk}}(k) &= \sum_{i=1}^{P} C_i\frac{1}{1-p_iz_0^k}\left\{1+\frac{1-(p_iz_0^k)^N}{N\{1-(p_iz_0^k)^{-1}\}}\right\} \\ &\quad +\frac{1}{N}\sum_{m=1}^{M-1}\sum_{i=1}^{P}C_ip_i^{mN}\frac{\{1-(p_iz_0^k)^N\}\{1-(p_iz_0^k)^{-N}\}}{(1-p_iz_0^k)\{1-(p_iz_0^k)^{-1}\}}z_0^{kmN} \\ &= \frac{1}{N}\sum_{i=1}^{P}C_i\frac{1}{(1-p_iz_0^k)\{1-(p_iz_0^k)^{-1}\}} \\ &\quad \times\Bigg[N\{1-(p_iz_0^k)^{-1}\}+1-(p_iz_0^k)^N \\ &\quad +\{1-(p_iz_0^k)^N\}\{1-(p_iz_0^k)^{-N}\}\sum_{m=1}^{M-1}(p_iz_0^k)^{Nm}\Bigg]. \quad (D.2)\end{aligned}$$

Since the last term $\sum_{m=1}^{M-1}(p_iz_0^k)^{Nm}$ in the last equation is equal to

$$\sum_{m=1}^{M-1}(p_iz_0^k)^{Nm} = (p_iz_0^k)^N\frac{1-(p_iz_0^k)^{(M-1)N}}{1-(p_iz_0^k)^N} \quad (D.3)$$

the term in the square brackets $[\cdot]$ of (D.2) is rearranged as follows:

$$\begin{aligned}[\,\cdot\,] &= N\{1-(p_iz_0^k)^{-1}\}+1-(p_iz_0^k)^N \\ &\quad +\{1-(p_iz_0^k)^{-N}\}(p_iz_0^k)^N\{1-(p_iz_0^k)^{(M-1)N}\} \\ &= N\{1-(p_iz_0^k)^{-1}\}+(p_iz_0^k)^{(M-1)N}\{1-(p_iz_0^k)^N\}. \quad (D.4)\end{aligned}$$

Thus, the estimate $\widehat{H_{bk}}(k)$ of the total transfer system obtained by the proposed method is given by

$$\begin{aligned}\widehat{H_{bk}}(k) &= \sum_{m=0}^{M-1}\widehat{H_m}(k)\exp\left(-j2\pi\frac{km}{M}\right) \\ &= \sum_{i=1}^{P}\frac{C_i}{1-p_iz_0^k}\left[1+\frac{(p_iz_0^k)^{(M-1)N}\{1-(p_iz_0^k)^N\}}{N\{1-(p_iz_0^k)^{-1}\}}\right]. \quad (D.5)\end{aligned}$$

This expression is used in (32) of the text.

ACKNOWLEDGMENT

The authors would like to thank Dr. K. Kido of Chiba Institute of Technology and Dr. H. Suzuki, Dr. K. Yamaguchi, H. Imaizumi, and Dr. M. Ohashi of Ono Sokki Co., Ltd. for their effective discussion.

REFERENCES

[1] J. W. Cooley and J. W. Tukey, "An algorithm for the machine calculation of complex Fourier series," *Math. Computat.*, vol. 19, no. 90, pp. 297–301, 1965.
[2] P. I. Richards, "Computing reliable power spectra," *IEEE Spectrum*, vol. 4, no. 1, pp. 83–90, 1967.
[3] W. T. Cochran *et al.*, "What is the fast Fourier transform?," *IEEE Trans. Audio Electroacoust.*, vol. AU-15 no. 2, pp. 45–55, 1967.
[4] C. Bingham, M. D. Godfrey, and J. W. Turkey, "Modern techniques of power spectrum estimation," *IEEE Trans. Audio Electroacoust.*, vol. AU-15, no. 2, pp. 56–66, 1967.
[5] P. D. Welch, "The use of fast Fourier transform for the estimation of power spectra: A method based on time averaging over short, modified periodgrams," *IEEE Trans. Audio Electroacoust.*, vol. AU-15, no. 2, pp. 70–73, 1967.
[6] G. M. Jenkins and D. G. Watts, *Spectral Analysis and Its Applications*. San Francisco: Holden-Day, 1968.
[7] V. A. Benignus, "Estimation of the coherence spectrum and its confidence interval using the fast Fourier transform," *IEEE Trans. Audio Electroacoust.*, vol. AU-17, no. 2, pp. 145–150, 1969.
[8] S. Bertram, "On the derivation of the fast Fourier transform," *IEEE Trans. Audio Electroacoust.*, vol. AU-18, no. 1, pp. 55–58, 1970.
[9] T. H. Glisson, C. I. Black, and A. P. Sage, "The digital computation of discrete spectra using the fast Fourier transform," *IEEE Trans. Audio Electroacoust.*, vol. AU-18, no. 3, pp. 271–287, 1970.
[10] J. W. Cooley, P. A. W. Lewis, and P. D. Welch, "The fast Fourier transform algorithm: Programming considerations in the calculation of sine, cosine, and Laplace transforms," *J. Sound Vibration*, vol. 12, no. 3, pp. 315–337, 1970.
[11] ——, "The application of the fast Fourier transform algorithm to the estimation of spectra and cross-spectra," *J. Sound Vibration*, vol. 12, no. 3, pp. 339–352, 1970.
[12] S. Bertram, "Frequency analysis using the discrete Fourier transform," *IEEE Trans. Audio Electroacoust.*, vol. AU-18, no. 4, pp. 495–500, 1970.
[13] J. S. Bendat and A. G. Piersol, *Random Data: Analysis and Measurement Procedures*. New York: Wiley, 1971.
[14] P. R. Roth, "Effective measurements using digital signal analysis," *IEEE Spectrum*, vol. 8, pp. 62–70, Apr. 1971.
[15] E. J. Hannan and P. J. Thomson, "The estimation of coherence and group delay," *Biometrika*, vol. 58, pp. 469–481, 1971.
[16] A. Eberhard, "An optimal discrete window for the calculation of power spectra," *IEEE Trans. Audio Electroacoust.*, vol. AU-21, no. 1, pp.

37–43, 1973.

[17] G. C. Carter, C. H. Knapp, and A. H. Nuttall, "Estimation of the magnitude-squared coherence function via overlapped fast Fourier transform processing," *IEEE Trans. Audio Electroacoust.*, vol. AU-21, no. 4, pp. 337–344, 1973.

[18] G. C. Carter, A. H. Nuttall, and P. G. Cable, "The smoothed coherence function (SCOT)," *Proc. IEEE*, vol. 61, no. 10, pp. 1497–1498, 1973.

[19] A. V. Oppenheim and R. W. Schafer, *Digital Signal Processing*. Englewood Cliffs, NJ: Prentice-Hall, 1975.

[20] G. C. Carter and C. H. Knapp, "Coherence and its estimation via the partitioned modified chirp z transform," *IEEE Trans. Acoust. Speech Signal Processing*, vol. ASSP-23, no. 3, pp. 257–264, 1975.

[21] C. J. Dodds and J. D. Robson, "Partial coherence in multivariate random processes," *J. Sound Vibration*, vol. 42, no. 2, pp. 243–249, 1975.

[22] C. R. S. Talbot, "Coherence function effects on phase difference determination," *J. Sound Vibration*, vol. 39, no. 3, pp. 345–358, 1975.

[23] A. H. Nuttall, "Estimation of cross-spectra via overlapped fast Fourier transform processing," NUSC Tech. Rep., 4169-S, Naval Underwater Syst. Cent., New London Laboratory, July 11, 1975.

[24] J. S. Bendat, "Solutions for the multiple input/output problem," *J. Sound Vibration*, vol. 44, no. 3, pp. 311–325, 1976.

[25] C. H. Knapp and G. C. Carter, "The generalized correlation method for estimation of time delay," *IEEE Trans. Acoust. Speech Signal Processing*, vol. ASSP-24, no. 4, pp. 320–327, 1976.

[26] H. Babic and G. C. Temes, "Optimum low-order windows for discrete Fourier transform systems," *IEEE Trans. Acoust. Speech Signal Processing*, vol. ASSP-24, no. 6, pp. 512–517, 1976.

[27] J. S. Bendat, "System identification from multiple input/output data," *J. Sound Vibration*, vol. 49, no. 3, pp. 293–308, 1976.

[28] W. K. Blake and R. V. Waterhouse, "The use of cross-spectral density measurements in partially reverberant sound fields," *J. Sound Vibration*, vol. 54, no. 4, pp. 589–599, 1977.

[29] C. K. Yuen, "A comparison of five methods for computing the power spectrum of a random process using data segmentation," *Proc. IEEE*, vol. 65, no. 6, pp. 984–986, 1977.

[30] F. J. Harris, "On the use of windows for harmonic analysis with the discrete Fourier transform," *Proc. IEEE*, vol. 66, no. 1, pp. 51–83, 1978.

[31] A. G. Piersol, "Use of coherence and phase data between two receivers in evaluation of noise environments," *J. Sound Vibration*, vol. 56, no. 2, pp. 215–228, 1978.

[32] T. M. Romberg, "An algorithm for the multivariate spectral analysis of linear system," *J. Sound Vibration*, vol. 59, no. 3, pp. 395–404, 1978.

[33] J. S. Bendat, "Statistical errors in measurement of coherence functions and input/output quantities," *J. Sound Vibration*, vol. 59, no. 3, pp. 405–421, 1978.

[34] A. F. Seybert and J. F. Hamilton, "Time delay bias errors in estimating frequency response and coherence functions," *J. Sound Vibration*, vol. 60, no. 1, pp. 1–9, 1978.

[35] S. Barrett, "On the use of coherence functions to evaluate sources of dynamic excitation," *Shock Vibration Bull.*, no. 49, pt. 1, pp. 43–58, 1979.

[36] J. S. Bendat and A. G. Piersol, *Engineering Applications of Correlation and Spectral Analysis*. New York: Wiley, 1980.

[37] A. H. Nuttall and G. C. Carter, "A generalized framework for power spectral estimation," *IEEE Trans. Acoust. Speech Signal Processing*, vol. ASSP-28, no. 3, pp. 334–335, 1980.

[38] Y. T. Chan, J. M. Riley, and J. B. Plant, "A Wiener filter approach to coherence estimation," in *Proc. IEEE Int. Conf. Acoust. Speech Signal Processing* (Denver, CO), Mar. 1980, pp. 646–649.

[39] N. R. Strader, II, "Effects of subharmonic frequencies on DFT coefficients," *Proc. IEEE*, vol. 68, no. 2, pp. 285–286, 1980.

[40] R. J. Webster, "Leakage regulation in the discrete Fourier transform spectrum," *Proc. IEEE*, vol. 68, no. 10, pp. 1339–1341, 1980.

[41] G. C. Carter and A. H. Nuttall, "On the weighted overlapped segment averaging method for power spectral estimation," *Proc. IEEE*, vol. 68, no. 10, pp. 1352–1354, 1980.

[42] A. W. Walker, "The effect of bandwidth on the accuracy of transfer function measurements of single degree of freedom response to random excitation," *J. Sound Vibration*, vol. 74, no. 2, pp. 251–263, 1981.

[43] A. H. Nuttall, "Some windows with very good side lobe behavior," *IEEE Trans. Acoustics Speech Signal Processing*, vol. ASSP-29, no. 1, pp. 84–91, 1981.

[44] K. Scarbrough, N. Ahmed, and G. C. Carter, "On the simulation of a class of time delay estimation algorithms," *IEEE Trans. Acoust. Speech Signal Processing*, vol. ASSP-29, no. 3, pp. 534–540, 1981.

[45] D. H. Youn, N. Ahmed, and G. C. Carter, "On using the LMS algorithm for time delay estimation," *IEEE Trans. Acoust. Speech Signal Processing*, vol. ASSP-30, no. 5, pp. 798–801, 1982.

[46] A. H. Nuttall and G. C. Carter, "Spectral estimation using combined time and lag weighting," *Proc. IEEE*, vol. 70, no. 9, pp. 1115–1125, 1982.

[47] D. H. Youn, N. Ahmed, and G. C. Carter, "Magnitude squared coherence function estimation: An adaptive approach," *IEEE Trans. Acoust. Speech Signal Processing*, vol. ASSP-31, no. 1, pp. 137–142, 1983.

[48] Y. T. Chan and R. K. Miskowisz, "Estimation of coherence function and time delay with ARMA models," *IEEE Trans. Acoust. Speech Signal Processing*, vol. ASSP-32, pp. 295–303, 1984.

[49] H. Schmidt, "Resolution bias errors in spectral density, frequency response and coherence function measurements I–VI," *J. Sound Vibration*, vol. 101, no. 3, pp. 347–427, 1985.

[50] G. C. Carter, "Coherence and time delay estimation," in *Proc. Ecole d'été de physique théorique Traitement du Signal Processing* (Les Houches, Haute Savoie, France), 1985, pp. 514–571.

[51] J. A. Cadzow and O. M. Solomon, Jr., "Linear modeling and the coherence function," *IEEE Trans. Acoust. Speech Signal Processing*, vol. ASSP-35, no. 1, pp. 19–28, 1987.

[52] V. J. Mathews, D. H. Youn, and N. Ahmed, "A unified approach to nonparametric spectrum estimation algorithms," *IEEE Trans. Acoust. Speech Signal Processing*, vol. ASSP-35, no. 3, pp. 228–349, 1987.

[53] C.-Y. Chi, D. Long, and F-K. Li, "Roundoff Noise analysis for digital signal power processors using Welch's power spectrum estimation," *IEEE Trans. Acoust. Speech Signal Processing*, vol. ASSP-35, no. 6, pp. 784–795, 1987.

[54] H. Gish and D. Cochran, "Invariance of the magnitude-squared coherence estimate with respect to second-channel statistics," *IEEE Trans. Acoust. Speech. Signal Processing*, vol. ASSP-35, no. 12, pp. 1774–1779, 1987.

[55] G. C. Carter, "Coherence and time delay estimation," *Proc. IEEE*, vol. 75, no. 2, pp. 236–255, 1987.

[56] M. G. Amin, "A new approach to recursive Fourier transform," *Proc. IEEE*, vol. 75, no. 11, pp. 1537–1538, 1987.

[57] G. L. Mohnkern, "Maximum likelihood estimation of magnitude-squared coherence," *IEEE Trans. Acoust. Speech Signal Processing*, vol. 36, no. 1, pp. 130–132, 1988.

[58] R. Cusani, "Performance of fast time delay estimators," *IEEE Trans. Acoust. Speech Signal Processing*, vol. 37, no. 5, pp. 757–759, 1989.

[59] D. Mansour and B. H. Juang, "The short-time modified coherence representation and noisy speech recognition," *IEEE Trans. Acoust. Speech Signal Processing*, vol. 37, no. 6, pp. 795–804, 1989.

[60] T. Ono, M. Ohashi, and H. Suzuki, "A new method for the determination of an optimum window length in frequency response function estimation," *in Proc. Amer. Soc. Mech. Eng. Pressure Vessels Piping Conf.*, vol. 177, pp. 233–238, 1989.

[61] T. Ono, M. Ohashi, T. Maeda, and H. Kanai, "Estimation of the damping factor of a signal transmission system by use of a delayed block coherence function," *J. Acoust. Soc. Japan*, vol. 46, no. 3, pp. 220–228, 1990 (in Japanese).

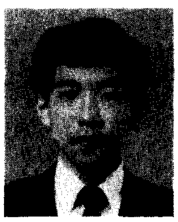

Hiroshi Kanai (A'89–M'91) was born in Matsumoto, Japan, on November 29, 1958. He received the B.E. degree from Tohoku University, Sendai, Japan in 1981 and the M.E. and the Dr. Eng. degrees, also from Tohoku University, in 1983 and 1986, both in electrical engineering.

From 1986 to 1988, he was with the Education Center for Information Processing, Tohoku University, as a Research Associate. From 1990 to 1992, he was a Lecturer at the Department of Electrical Engineering, Faculty of Engineering, Tohoku University. Since 1992, he has been an Associate Professor at the Department of Electrical Engineering, Faculty of Engineering, Tohoku University. His present interest is in digital signal processing and its application on the acoustical, ultrasonic, and electrical measurements.

Dr. Kanai is a member of the Acoustical Society of Japan, the Institute of Electronics Information and Communication Engineering of Japan, the Japan Society of Mechanical Engineers, the Japan Society of Ultrasonics in Medicine, the Japan Society of Medical Electronics and Biological Engineering, the Institute of Electrical Engineers of Japan, and the Japanese Circulation Society.

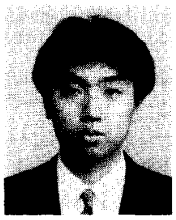

Toyohiko Hori was born in Toyama, Japan on March 5, 1969. He graduated from Tohoku University, Sendai, Japan, in 1992.

Since 1992, he has been with NTT, Japan. His interest is in digital signal processing and its application to acoustical measurements.

Noriyoshi Chubachi (M'83) was born in Kokura, Japan, on October 5, 1933. He received the B.S., M.S., and Ph.D. degrees in electrical engineering from Tohoku University, Sendai, Japan, in 1956, 1962, and 1965, respectively.

In 1965, he joined the Research Institute of Electrical Communication, Tohoku University, where he was an Associate Professor from 1966 to 1978. Since 1979, he has been a Professor at the Department of Electrical Engineering, Tohoku University. From 1982 to 1983, he was a visiting Professor of Electrical and Computer Engineering, University of California, Santa Barbara. He has worked on ultrasonic transducers and delay lines, surface acoustic devices, acoustoelectronics, piezoelectric materials, acoustic microscopy, and related problems.

Dr. Chubachi is a member of the Institute of Electronics and Communication Engineers of Japan, the Society of Japanese Applied Physics, the Acoustical Society of Japan, the Japan Society of Ultrasonics in Medicine, the Japan Society for Nondestructive Inspection, the Japan Society of Medical Electronics and Biological Engineering, the Japan Society of Mechanical Engineers, and the Institute of Electrical Engineers of Japan. He served as chairman, Tokyo chapter of IEEE UFFC Society from 1987 to 1988.

Takahiko Ono was born in Yokohama, Japan, in September, 1951. He received the B.A. degree from Keio University, Faculty of Business and Commerce, Tokyo, Japan, in 1974. In 1989, he received the Dr. Eng. Degree in electrical engineering from Tohoku University, Sendai, Japan.

In 1976, he joined Ono Sokki Co., Ltd. as the product planning engineer and was named a member of the board in 1983. Since 1991, he has been the President and Chief Executive Officer of Ono Sokki Co., Ltd. Besides his business, he is now a part-time teacher at Tokyo University of Agriculture and Technology.

He is a member of the Japan Society of Mechanical Engineering and the Acoustical Society of Japan.